Smart Structures and Systems, Vol. 2, No. 2 (2006) 127-140
DOI: http://dx.doi.org/10.12989/sss.2006.2.2.127

Covariance-driven wavelet technique for structural damage assessment

Z. Sun†

State Key Laboratory for Disaster Reduction in Civil Engineering, Tongji University, Shanghai, China

C. C. Chang‡

Department of Civil Engineering, Hong Kong University of Science and Technology, Clear Water Bay, Kowloon, Hong Kong

(Received March 14, 2005, Accepted December 7, 2005)

Abstract. In this study, a wavelet-based covariance-driven system identification technique is proposed for damage assessment of structures under ambient excitation. Assuming the ambient excitation to be a white-noise process, the covariance computation is shown to be able to separate the effect of random excitation from the response measurement. Wavelet transform (WT) is then used to convert the covariance response in the time domain to the WT magnitude plot in the time-scale plane. The wavelet coefficients along the curves where energy concentrated are extracted and used to estimate the modal properties of the structure. These modal property estimations lead to the calculation of the stiffness matrix when either the spectral density of the random loading or the mass matrix is given. The predicted stiffness matrix hence provides a direct assessment on the possible location and severity of damage which results in stiffness alteration. To demonstrate the proposed wavelet-based damage assessment technique, a numerical example on a 3 degree-of-freedom (DOF) system and an experimental study on a three-story building model, which are all under a broad-band excitation, are presented. Both numerical and experimental results illustrate that the proposed technique can provide an accurate assessment on the damage location. It is however noted that the assessment of damage severity is not as accurate, which might be due to the errors associated with the mode shape estimations as well as the assumption of proportional damping adopted in the formulation.

Keywords: wavelet transform; covariance response; modal identification; damage assessment.

1. Introduction

Structure modal parameters, such as resonant frequencies and mode shape vectors, are the most commonly used condition indices for global vibration-based structural health monitoring and damage detection techniques. Accurate determination of these parameters is one important step toward the success of detecting, locating and quantifying structural damage for these global vibration-based techniques. These modal properties traditionally have been obtained from temporal signals via the Fourier transform (FT). There are a few inherent characteristics of FT that might affect the accuracy of modal property

†Associate Professor, Corresponding Author, Email: sunzhi1@mail.tongji.edu.cn
‡Associate Professor, Email: cechang@ust.hk.

estimation. The FT decomposes a temporal signal into superposition of stationary harmonic functions. As a result, it is not able to preserve the time dependency that might have existed in the signal and hence it can not capture the evolutionary characteristics that are commonly observed in the signals measured from naturally-excited structures.

Wavelet transform (WT) is a novel signal processing technique that translates a temporal signal into a time-scale plane through dilating and translating of a chosen mother wavelet. While the dilation of the mother wavelet can be considered as a frequency filtering process, the translation along the time axis preserves the time dependency of the signal. As a result, the WT can capture both stationary and transient information from the original signal. Staszewski (1997) used the WT to estimate the damping ratio from the impulse response of a multi-degree-of-freedom (MDOF) system. Ruzzene, *et al.* (1997) used the WT to process the free vibration response of a MDOF system to estimate their natural frequencies and damping ratios. For ambient excitation, random decrement technique was used to extract the impulse response from the measurements prior to applying the WT. Piomo, *et al.* (2000) developed a WT technique to estimate the mode shape vector and proposed a modal quality index to evaluate the reliability of the estimation. Kijewski and Kareem (2003) discussed the time and frequency resolutions of the wavelet based system identification method and showed the way to insure the modal separation and to minimize the end-effect errors. Chang, *et al.* (2003) verified the efficiency and accuracy of a WT based modal parameter estimation technique through an experimental study. Note that the WT based system identification techniques reviewed above were all performed on structural impulse response function or free vibration response. As civil engineering structures are generally subjected to ambient excitation, such as traffic, wind or earthquake, which have random characteristics and generally immeasurable, it is necessary to develop some output-only technique under such a condition. Peeters and Roeck (2001) performed a review on operational modal analysis and presented that since the output covariances (of a system excited by white noise) have the similar mathematical expressions as system impulse responses, it is logical to feed the impulse response based modal parameter estimation methods with output covariances instead to deal with the operational modal analysis problem in time domain.

In this paper, a wavelet-based covariance-driven system identification technique is proposed for damage assessment of structures under ambient excitation. Assuming the ambient excitation to be a white-noise process, the covariance of structural response is shown to be able to separate the effect of random excitation from the response measurement. WT is then used to convert the response covariance in the time domain to the WT magnitude plot in the time-scale plane. The wavelet coefficients along the energy concentrated curves can be extracted and used to estimate the modal properties of the structure. These modal property estimations can lead to the calculation of the stiffness matrix when either the spectral density of the random loading or the mass matrix is given. This predicted stiffness matrix hence provides a direct assessment on the possible location and severity of damage which results in stiffness alteration. To demonstrate the proposed wavelet-based damage assessment technique, a numerical example on a three-story shear-beam model and an experimental study on a three-story frame structure under a broad-band excitation are presented.

2. Formulation

2.1. Covariance analysis

Assume that an n-degree-of-freedom (n-DOF) structure is excited by a random force f. The equations of motion for this structure can be expressed as,

$$\boldsymbol{M}\ddot{\boldsymbol{Z}} + \boldsymbol{C}\dot{\boldsymbol{Z}} + \boldsymbol{K}\boldsymbol{Z} = \boldsymbol{D}f \tag{1}$$

where $\boldsymbol{M}$, $\boldsymbol{C}$ and $\boldsymbol{K}$ are the mass, damping and stiffness matrices of the structure, respectively; $\boldsymbol{D}$ is the force location vector; and $\boldsymbol{Z} = [z_1 z_2 \cdots z_n]^T$ is the displacement vector where z_i is the displacement response of the i-th degree. Since the structures concerned in this study are those with similar and distributed damping mechanism, they are thus assumed to be proportionally damped. Under this assumption, structural displacement response can be expressed in the form of modal superposition as,

$$\boldsymbol{Z} = \sum_{j=1}^{n} \boldsymbol{\Phi}_j q_j \tag{2}$$

where $\boldsymbol{\Phi}_j$ and q_j are the mode shape vector and the generalized modal coordinate for the jth mode, respectively. The decoupled equation of motion for the jth mode can be expressed as

$$\ddot{q}_j + 2\zeta_j \omega_j \dot{q}_j + \omega_j^2 q_j = \frac{d_j}{m_j} f \tag{3}$$

where ω_j, ζ_j, and m_j are the natural frequency, damping ratio and modal mass for the jth mode, respectively; and the jth modal participation factor $d_j = \boldsymbol{\Phi}_j^T \boldsymbol{D}$. Assuming that the force f is a zero-mean Gaussian white noise with a constant spectral intensity of S_0, the steady-state auto-covariance of q_j, denoted as R_j, can be expressed as

$$R_j(t) = B_j e^{-\zeta_j \omega_j t} \cos(\overline{\omega}_j t - \theta_j) \tag{4}$$

$$B_j = \frac{\pi d_j^2 S_0}{2 m_j^2 \zeta_j \omega_j^3}, \quad \overline{\omega}_j = \omega_j \sqrt{1 - \zeta_j^2}, \quad \theta_j = \tan^{-1} \frac{\zeta_j}{\sqrt{1 - \zeta_j^2}} \tag{5a, b, c}$$

where $\overline{\omega}_j$ is the jth damped frequency and θ_j is a phase angle related to damping.

The steady-state cross-covariance response between the g-th DOF and the h-th DOF of the structure R_{gh} can be approximately obtained following Eq. (2)

$$R_{gh}(t) \cong \sum_{j=1}^{n} \phi_j^g \phi_j^h R_j(t) \tag{6}$$

where ϕ_j^g and ϕ_j^h are the g-th and the h-th element of the jth mode shape vector. Note that in this equation, the cross-covariance terms between different modes have been neglected. This is applicable when the natural frequencies are distinctly separated and the damping ratios are small such that the following inequality is satisfied: $|\omega_i - \omega_j| \gg \max\{\zeta_i \omega_i, \zeta_j \omega_j\}$ for $i \neq j$.

When the discrete time responses at the g-th DOF and the h-th DOF are measured and available, the cross-covariance response R_{gh} on the left-hand side of Eq. (6) can be estimated by,

$$R_{gh}(i\Delta t) \cong \frac{1}{N}\sum_{n=1}^{N} z_g(n\Delta t)z_h[(n+i)\Delta t] \qquad i = 0, 1, 2, \ldots \tag{7}$$

where N is the total number of data points and Δt is the time increment. Note that this estimation can also be achieved by averaging over a few samples of measured responses with limited time duration. It is however essential to ensure the convergence of the cross-covariances using either a sufficient amount of data points or samples.

2.2. Wavelet based modal identification

WT is a time-frequency domain signal processing technique that converts a time-domain square-integrable $x(t)$ signal into the time-scale plane (a,t) according to

$$W_x(a, t) = \frac{1}{\sqrt{a}}\int_{-\infty}^{\infty} x(\tau)\,\psi^*\left(\frac{t-\tau}{a}\right)d\tau \tag{8}$$

where * denotes the complex conjugation; a is a scale parameter controlling the stretch of analysis window; and $W_x(a,t)$ is the wavelet coefficient of signal $x(t)$. The mother wavelet $\psi(t)$ is a wave function that has a limited duration and an average value of zero. In this study, one notable Gaussian mother wavelet, the Morlet wavelet, is used:

$$\psi(t) = e^{i\omega_0 t}e^{-t^2/2} \tag{9}$$

where ω_0 is the central frequency for the Morlet wavelet.

Performing the WT on both sides of Eq. (6) results in

$$W_{R_{gh}}(a, t) = \sum_{j=1}^{n} \phi_j^g \phi_j^h W_{R_j}(a, t) \tag{10}$$

where the WT coefficient of the auto-covariance of the jth modal response W_{R_j} can be approximated as follows when R_j is an asymptotic signal (Delprat, *et al.* 1992),

$$W_{R_j}(a, t) = \sqrt{a}B_j e^{-\zeta_j\omega_j t}e^{-(a\varpi_j-\omega_o)^2}e^{i(\varpi_j t-\theta_j)} \tag{11}$$

Substituting Eq. (11) into Eq. (10) and taking magnitude on both sides give

$$\left|W_{R_{gh}}(a, t)\right| = \sum_{j=1}^{n} \left|\phi_j^g\right|\left|\phi_j^h\right|\sqrt{a}B_j e^{-\zeta_j\omega_j t}e^{-(a\varpi_j-\omega_o)^2} \tag{12}$$

It can be seen from this equation that for a structure with distinct damped frequencies, the magnitude of wavelet coefficients of the cross-covariance R_{gh} should have n distinct local maximums along the scale axis at any time instance. These local maximal scales or the so-called ridges keep constant along time for a linear structure with constant properties. In this study, these ridge scales are extracted by searching for the local maximum at any given time on pre-selected scalar regions of the wavelet magnitude plot. These scalar regions can be selected by observing the wavelet magnitude plot. From Eq. (12), these ridges correspond to

$$a_j = \frac{\omega_o}{\omega_j}, \qquad j = 1, 2, \ldots, n \tag{13}$$

Also, as the damped frequencies are distinctly different, Eq. (12) can be further approximately written at the jth ridge as,

$$W_{R_{gh}}(a_j, t) \cong \phi_j^g \phi_j^h \sqrt{a_j}\, B_j e^{-\zeta_j \omega_j t} e^{i(\overline{\omega}_j t - \theta_j)} \tag{14}$$

Based on this equation, the following two formulas can be obtained,

$$-\zeta_j \omega_j \cong \frac{d}{dt} \ln \left| W_{R_{gh}}(a_j, t) \right| \tag{15}$$

$$\overline{\omega}_j = \omega_j \sqrt{1 - \zeta_j^2} \cong \frac{d}{dt}(\angle W_{R_{gh}}(a_j, t)) \tag{16}$$

These two simultaneous equations can be used to determine the jth natural frequency ω_j and damping ratio ζ_j. In principle, wavelet coefficients of only one cross-covariance or auto-covariance are required to obtain the n distinct natural frequencies and damping ratios. To estimate the mode shape vectors, it is necessary to have both the auto-covariance at a reference location and cross-covariances between the reference and the other locations. From Eq. (14), it is not difficult to see that the jth mode shape ratio between location h and location g follows this relation,

$$\frac{\phi_j^h}{\phi_j^g} \cong \frac{W_{R_{gh}}(a_j, t)}{W_{R_{gg}}(a_j, t)} \tag{17}$$

2.3. Stiffness estimation

When either the mass matrix or the spectral density of the random loading is given, the modal property estimations outlined above can further lead to the calculation of the stiffness matrix. This updated stiffness matrix hence provides a way for assessing the location and the severity of damage that might have existed in the structure. Assuming that the mass matrix, which tends not to be affected by the presence of damage, is available, the jth modal mass and modal stiffness can be estimated by

$$m_j = \phi_j^T M \phi_j; \quad k_j = m_j \omega_j^2 \tag{18a,b}$$

The stiffness matrix can then be obtained using Eq. (18b) and the mode shape vectors. If the spectral density of the random loading is given instead of the mass matrix, the jth modal mass can be obtained from Eq. (14) as,

$$m_j = \sqrt{\frac{\sqrt{a_j}\left|\phi_j^g\right|\left|\phi_j^h\right| \pi d_j^2 S_0}{2\zeta_j \omega_j^3 \left|W_{R_{gh}}(a_j, 0)\right|}} \tag{19}$$

The estimation of stiffness matrix then follows the same as outlined above.

3. Numerical demonstration

To demonstrate the proposed covariance-driven wavelet-based damage assessment technique, a numerical study on a three-story shear-beam model (as shown in Fig. 1) was performed. The mass and stiffness properties were assumed as m_1 = 1500 kg, $m_2 = m_3$ = 2500 kg, k_1 = 1.96 MN/m, $k_2 = k_3$ = 3.92 MN/m, respectively. The modal frequencies were computed to be 3.06, 7.00 and 10.66 Hz. The damping ratios were assumed to be 2% for all modes. Assume that a broad-band white noise excitation with a spectral intensity of 900 MN^{2}s was acting on the top floor of the building. The sampling frequency was set to be 50 Hz during the numerical simulation. The acceleration responses at all three floors were assumed to be available for analysis.

To estimate the natural frequencies and damping ratios, the response at the second floor was used. The auto-covariance for this response was first computed. The time duration of the covariance response was set at 6 seconds, which was long enough for the covariance response to decay 99% of its energy. To ensure the convergence of the auto-covariance, 500 simulations were performed under the same level of excitation. The converged covariance response is shown in Fig. 2(a). Performing FT and WT on the covariance response, the power spectrum density (PSD) and WT magnitude plot are obtained shown in Figs. 2(b) and 2(c), respectively. It is seen from the PSD plot that there are three distinct peaks which correspond to the three modes of the frame. In the WT magnitude plot, there are three dark areas where contours are concentrated along the scale axis. These three areas correspond to the three modes of the structure. As the scale is inversely proportional to the frequency, the top dark area (area A) corresponds to the 1st mode and the bottom dark area (area C) corresponds to the 3rd mode.

For modal parameter identification, the ridge scale corresponding to the energy concentrated curve was first extracted. The phase angle and modulus of the wavelet coefficient at this ridge scale could hence be obtained. Figs. 3(a) and 3(b) show the phase angle and modulus of the wavelet coefficient corresponding to the 1st mode. The solid lines in the figure are the linear regression of phase angle and the modulus envelop which can be used to estimate the modal parameters. Following this procedure, the natural frequencies are estimated to be 3.06, 7.00 and 10.64Hz and the damping ratios are 2.01%,

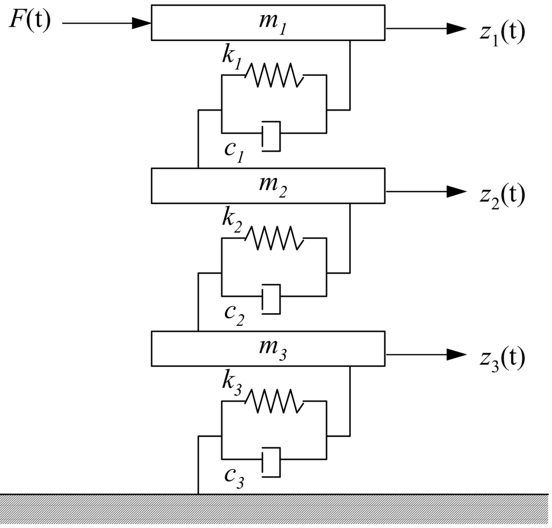

Fig. 1 A 3DOF system

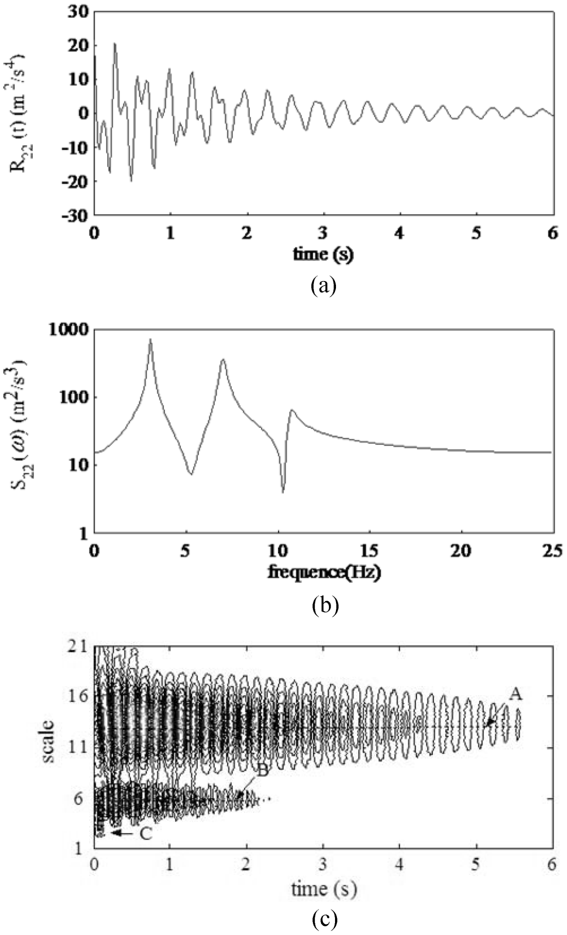

Fig. 2 (a) The converged acceleration covariance response with (b) its PSD plot and (c) wavelet domain power magnitude plot for the 3DOF system

2.02% and 2.00% (as shown in Table 1), respectively. The error of estimation is less than 0.2% for the natural frequencies and less than 1% for the damping ratios.

To estimate the mode shape vectors, responses at all three floors had to be measured. Selecting the 2nd floor as the reference location, the cross-covariances between other floors and the 2nd floor were computed along with the auto-covariances of the 2nd floors. The mode shape vectors of these three modes could hence be estimated using Eq. (17). The estimated mode shape vectors are plotted in Fig. 4. It is seen that the estimated mode shapes match very well with the analytical mode shapes. Also can be seen from Table 1, the maximum estimation error of the mode shape vectors is about 3.2% for the 3rd mode. This estimation error may be resulted from the approximation used in deriving Eq. (14) from Eq. (12). For those modes that have small WT coefficients, the effect from the other modes might be more pronounced hence might lead to larger error in the mode shape estimation. Assuming that the spectral density of the loading is known, the modal masses can be estimated using Eq. (19). The stiffness matrix of the system can then be calculated once the three modal stiffness coefficients are found from Eq. (18b). Table 1 lists the stiffness matrix obtained as well as the three element stiffness

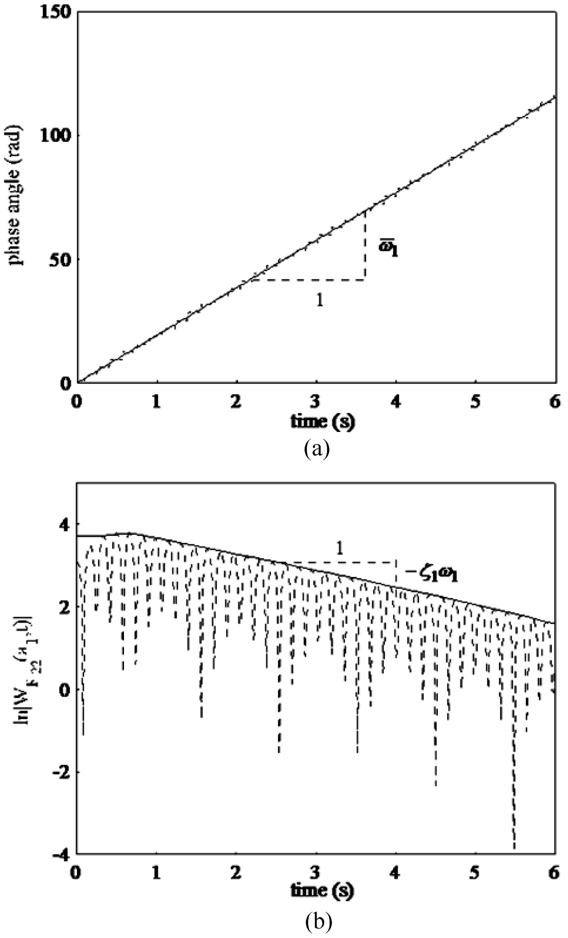

Fig. 3 (a) The phase angle and (b) modulus plot of the wavelet coefficient for the fundamental mode estimation

coefficients from the diagonal elements of the stiffness matrix. It is seen that the error of stiffness estimation is generally around 3%.

To test applicability of the method to damage assessment, three damaged cases are simulated. For damage cases 1 and 2, k_3 is reduced by 10% and 30% of the original value, respectively. For damage case 3, k_2 is reduced by 20%. Using the same procedure described above, the modal parameters and the stiffness matrix are estimated and shown in Table 2. It is seen that in general the location of damage can be quite correctly identified which is represented by a significant reduction of the element stiffness coefficient. For example, it is found for cases 1 and 2 that k_3 is reduced to 3.1 MN/m (case 1) and 2.5 MN/m (case 2) respectively from 3.9 MN/m while the other two stiffness coefficients remain pretty much unchanged. Similarly, for case 3, k_2 is reduced from 3.8 MN/m to 2.73 MN/m while the other two stiffness coefficients remain almost unchanged. Although the location of damage can be identified, it seems that the severity of damage is not as accurate. Results show that the 10% reduction of k_3 in case 1 is estimated to be about 20%, the 30% reduction of k_3 in case 2 is estimated to be about 35%, and the 20% reduction of k_2 in case 3 is estimated to be about 28%. The reason for this discrepancy is perhaps due to the errors associated with the mode shape estimations.

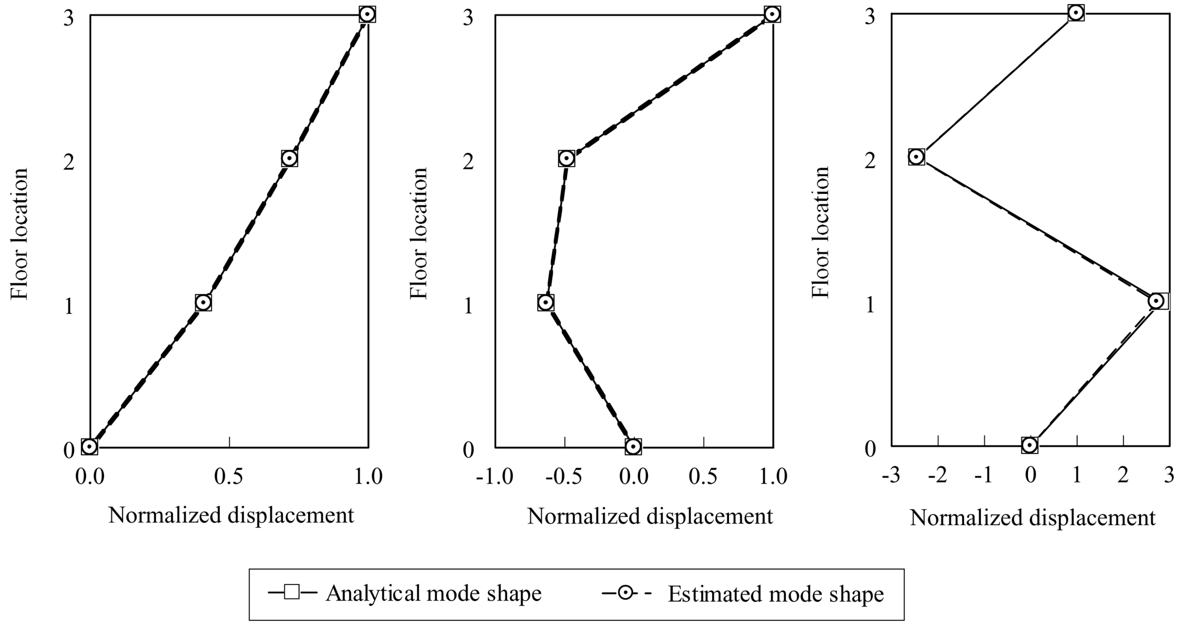

Fig. 4 Mode shape vectors of the 3DOF system

Table 1 Modal parameters for the 3-DOF system in healthy state

	ω (Hz)	$\boldsymbol{\Phi}$	$\boldsymbol{K}$ (MN/m)	$[k_1\ k_2\ k_3]$ (MN/m)
Analytical	[3.06 7.00 10.66]	$\begin{bmatrix} 100 & 1.00 & 1.00 \\ 0.72 & -0.48 & -2.44 \\ 0.41 & -0.63 & 2.82 \end{bmatrix}$	$\begin{bmatrix} 1.96 & -1.96 & 0 \\ -1.96 & 5.88 & -3.92 \\ 0 & -3.92 & 7.84 \end{bmatrix}$	$\begin{bmatrix} 1.96 & 3.92 & 3.92 \end{bmatrix}$
Estimated	[3.06 7.00 10.64]	$\begin{bmatrix} 1.00 & 1.00 & 1.00 \\ 0.72 & -0.48 & -2.45 \\ 0.41 & -0.63 & 2.73 \end{bmatrix}$	$\begin{bmatrix} 1.91 & -1.88 & 0' \\ -1.88 & 5.71 & -3.85 \\ 0 & -3.85 & 7.69 \end{bmatrix}$	$\begin{bmatrix} 1.96 & 3.80 & 3.89 \end{bmatrix}$

4. Experimental verification

To further verify the applicability of this damage assessment technique, an experimental study on a three-story metal frame (see Fig. 5a) was conducted. The frame was mounted on a shake table and excited by broad-band Gaussian white noise along one direction. Since the floor systems of the frame were greatly stiffer than its columns in flexure, the excitation was along one direction, and the axial deformation of the columns could be neglected, the frame was idealized as a two dimensional 3-story shear-beam frame as shown in Fig. 5(b). The three story masses were m_1=5.03 kg, m_2=6.64 kg and m_3= 6.69 kg, respectively. The columns consisted of two metal strips that were bolted together: one thicker strip was made of aluminum and the other thinner strip was made of steel. The cross sections of the

Table 2 Estimation results of the 3-DOF system for different damage conditions

	Healthy	Case 1	Case 2	Case 3
ω (Hz)	[3.06 7.00 10.64]	[2.97 6.89 10.56]	[2.75 6.70 10.36]	[2.94 6.98 9.91]
$\boldsymbol{\Phi}$	$\begin{bmatrix} 1.00 & 1.00 & 1.00 \\ 0.72 & -0.48 & -2.45 \\ 0.41 & -0.63 & 2.73 \end{bmatrix}$	$\begin{bmatrix} 1.00 & 1.00 & 1.00 \\ 0.74 & -0.44 & -2.32 \\ 0.45 & -0.65 & 2.71 \end{bmatrix}$	$\begin{bmatrix} 1.00 & 1.00 & 1.00 \\ 0.72 & -0.32 & -2.00 \\ 0.48 & -0.63 & 2.36 \end{bmatrix}$	$\begin{bmatrix} 1.00 & 1.00 & 1.00 \\ 0.74 & -0.52 & -2.10 \\ 0.37 & -0.67 & 2.40 \end{bmatrix}$
$\boldsymbol{K}$ (MN/m)	$\begin{bmatrix} 1.91 & -1.88 & 0 \\ -1.88 & 5.71 & -3.85 \\ 0 & -3.85 & 7.69 \end{bmatrix}$	$\begin{bmatrix} 1.97 & -2.00 & 0 \\ -2.00 & 5.90 & -3.85 \\ 0 & -3.85 & 7.03 \end{bmatrix}$	$\begin{bmatrix} 2.02 & -2.26 & 0.12 \\ -2.26 & 6.01 & -4.01 \\ 0.12 & -4.01 & 6.53 \end{bmatrix}$	$\begin{bmatrix} 1.86 & -1.75 & -0.12 \\ -1.75 & 4.59 & -2.77 \\ -0.12 & -2.77 & 6.70 \end{bmatrix}$
Estimated $[k_1\ k_2\ k_3]$ (MN/m)	$[1.91\ 3.80\ 3.89]$	$[1.97\ 3.93\ 3.10]$	$[2.02\ 3.99\ 2.54]$	$[1.86\ 2.73\ 3.99]$
Target $[k_1\ k_2\ k_3]$ (MN/m)	$[1.96\ 3.92\ 3.92]$	$[1.96\ 3.92\ 3.53]$	$[1.96\ 3.92\ 2.74]$	$[1.96\ 3.14\ 3.92]$

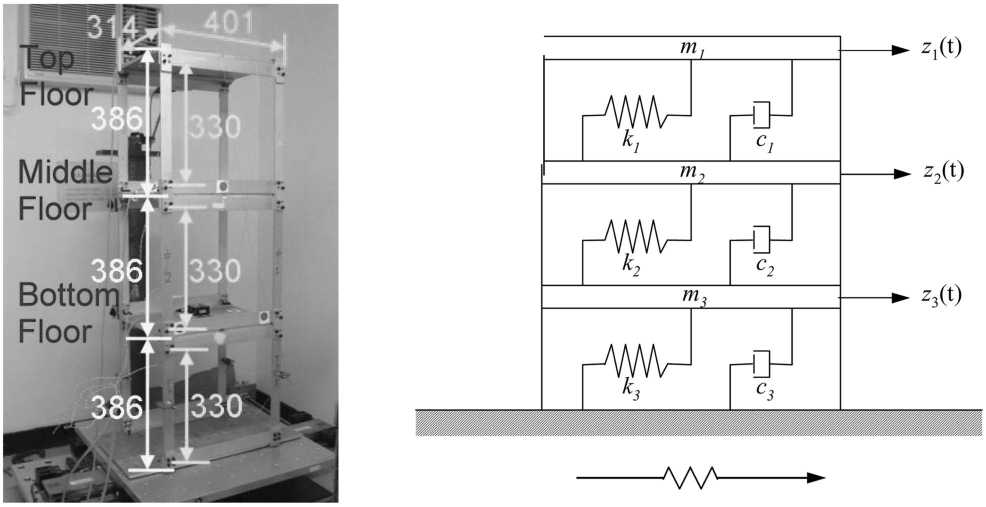

(a) (b)

Fig. 5 (a) A 3-story frame (b) the idealized shear beam analytical model

steel and alumni strips were rectangular with dimensions of 31.0 × 2.5 mm and 31.0 × 4.5 mm, respectively. The steel strips could be dismantled independently to simulate damage of story stiffness. The undamaged story stiffness was calculated to be 33.0 kN/m. When all four steel strips at a story were removed, the story stiffness reduced to 21.7 kN/m, which corresponded to a 34% reduction of the original story stiffness. Three damage cases were studied: (i) C1: the four steel strips at the bottom floor were removed; (ii) C2: the four steel strips at the middle floor were removed; and (iii) C3: the steel strips at both the bottom and the top floors were removed. Fig. 6 illustrates the damage locations for the three cases. For comparison, the healthy case was denoted as case C0. Three accelerometers were

Case 0 Case 1

Case 2 Case 3

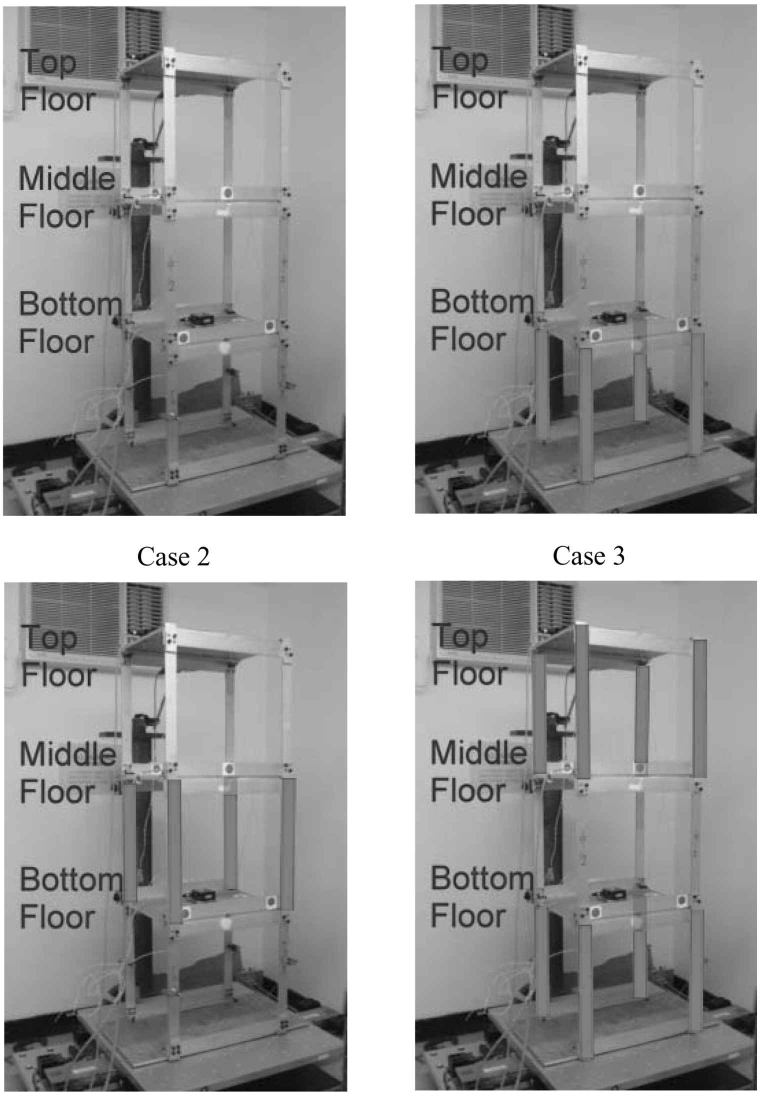

Fig. 6 Damage cases

installed on the three stories to measure the acceleration responses. The sampling frequency was set at 100 Hz during the signal acquisition.

Fig. 7 shows a typical white noise excitation record and the measured acceleration response at the 2nd story together with the computed covariance response. The natural frequencies and the damping ratios of this frame could then be estimated from the extracted WT phase angle and modulus plots as shown in Fig. 8. The three natural frequencies are estimated to be 5.0, 14.9 and 21.3 Hz respectively, while the corresponding damping ratios are 3.1%, 0.9% and 1.7% respectively. The stiffness matrix could be computed using Eq. (18) after the mode shape vectors were computed from Eq. (17). Similarly, the modal parameters and the stiffness matrices of the three damage cases could be computed following the

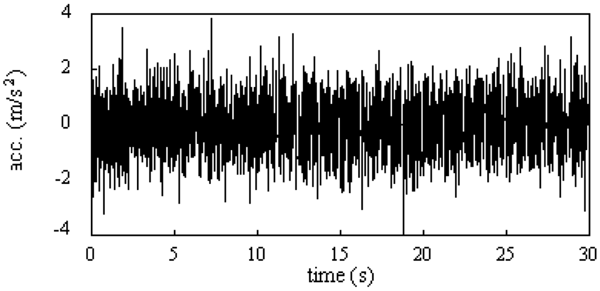

(a)

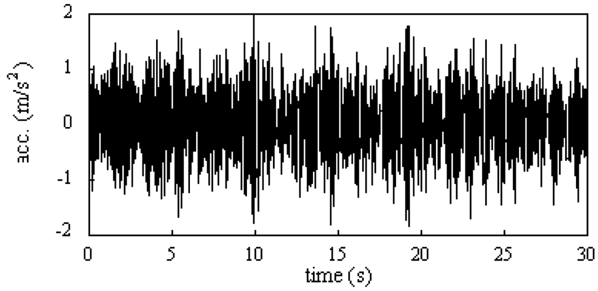

(b)

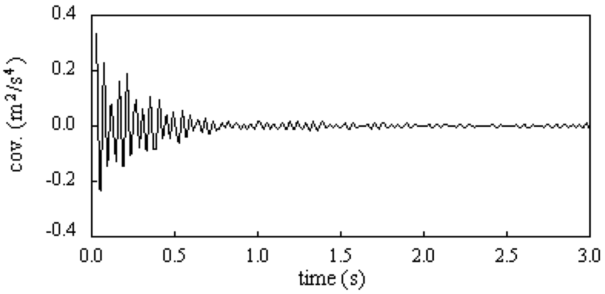

(c)

Fig. 7 (a) A typical white noise ground excitation, (b) the corresponding 2nd floor acceleration response and (c) the computed covariance response

same procedure. Table 3 summarizes the results obtained. It is seen from the estimated story stiffness coefficients that the damage locations of the three damage cases can all be correctly identified. These locations are identified by a significant reduction of story stiffness. For example, for case C1, the story stiffness k_3 is estimated to be 10.5 kN/m which is significantly different from that of the healthy condition (35.3 kN/m) while the other two story stiffness remained pretty much the same as that of the healthy condition. Similarly, the story stiffness k_2 is estimated to be 26.2 kN/m while the other two story stiffness remained almost unchanged. On the other hand, it is also seen that the estimation of stiffness coefficients is not as accurate. For example, the story stiffness k_2 is estimated to be 26.2 kN/m while the target value is 21.7 kN/m for case C2. For case C3, k_1 and k_3 are estimated to be 25.4 kN/m and 19.6 kN/m, respectively, while their target values are both 21.7 kN/m. These estimation errors could possibly be attributed to the errors associated with the assumption adopted during the frame modeling as well as the approximation adopted in the modal parameter estimation.

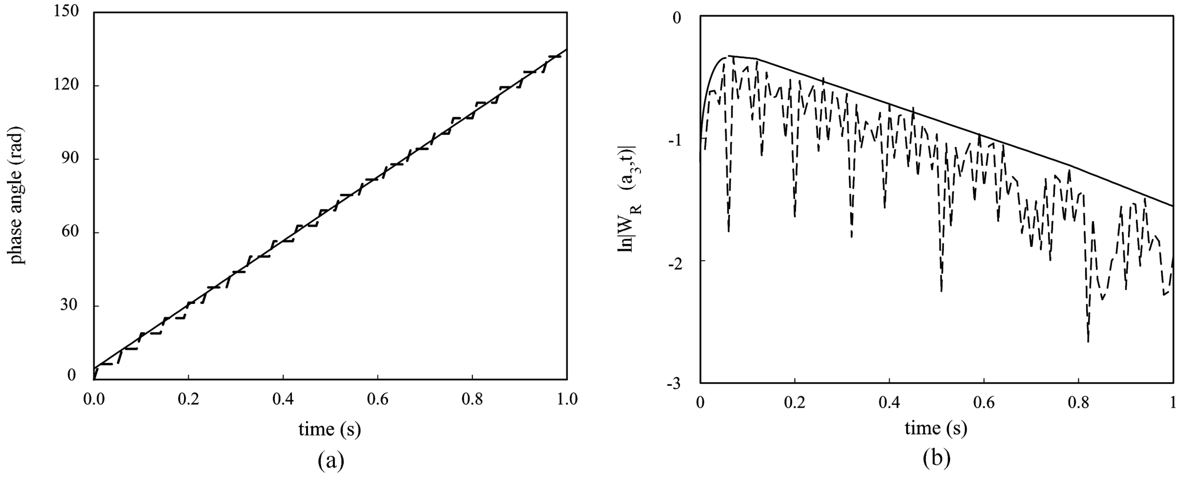

Fig. 8(a) The phase angle, and (b) the modulus plot of the wavelet coefficient for the third mode

Table 3 Estimation results of the frame for different damage conditions

	Case C0	Case C1	Case C2	Case C3
ω (Hz)	[5.01 14.91 21.31]	[4.05 13.20 20.40]	[4.76 14.81 19.69]	[3.94 12.00 18.50]
ζ (%)	[3.05 0.86 1.70]	[1.55 0.89 1.62]	[2.59 1.65 2.39]	[1.88 1.06 1.53]
$\boldsymbol{\Phi}$	$\begin{bmatrix} 1.00 & 1.00 & 1.00 \\ 0.84 & -0.34 & -1.79 \\ 0.46 & -1.02 & 1.49 \end{bmatrix}$	$\begin{bmatrix} 1.00 & 1.00 & 1.00 \\ 0.86 & -0.28 & -1.47 \\ 0.59 & -1.49 & 1.32 \end{bmatrix}$	$\begin{bmatrix} 1.00 & 1.00 & 1.00 \\ 0.82 & -0.26 & -1.15 \\ 0.38 & -2.09 & 0.38 \end{bmatrix}$	$\begin{bmatrix} 1.00 & 1.00 & 1.00 \\ 0.84 & -0.36 & -2.35 \\ 0.64 & -1.06 & 2.07 \end{bmatrix}$
$\boldsymbol{K}$ (kN/m)	$\begin{bmatrix} 34.6 & -36.0 & 1.4 \\ -36.0 & 69.1 & -36.2 \\ 1.4 & -36.2 & 69.9 \end{bmatrix}$	$\begin{bmatrix} 38.7 & -41.2 & 0.6 \\ -41.2 & 72.6 & -29.2 \\ 0.6 & -29.2 & 44.4 \end{bmatrix}$	$\begin{bmatrix} 34.5 & -35.7 & -1.1 \\ -35.7 & 60.7 & -24.6 \\ -1.1 & -24.6 & 60.6 \end{bmatrix}$	$\begin{bmatrix} 25.4 & -26.3 & 0.3 \\ -26.3 & 58.4 & -30.3 \\ 0.3 & -30.3 & 42.6 \end{bmatrix}$
Estimated $[k_1\ k_2\ k_3]$ (kN/m)	$\begin{bmatrix} 34.6 & 34.5 & 35.3 \end{bmatrix}$	$\begin{bmatrix} 38.7 & 33.9 & 10.5 \end{bmatrix}$	$\begin{bmatrix} 34.5 & 26.2 & 34.4 \end{bmatrix}$	$\begin{bmatrix} 25.4 & 33.0 & 19.6 \end{bmatrix}$
Target $[k_1\ k_2\ k_3]$ (kN/m)	$\begin{bmatrix} 33.0 & 33.0 & 33.0 \end{bmatrix}$	$\begin{bmatrix} 33.0 & 33.0 & 21.7 \end{bmatrix}$	$\begin{bmatrix} 33.0 & 21.7 & 33.0 \end{bmatrix}$	$\begin{bmatrix} 21.7 & 33.0 & 21.7 \end{bmatrix}$

5. Conclusions

A wavelet-based covariance-driven system identification technique is proposed in this study for damage assessment of structures under ambient excitation. Assuming the ambient excitation to be a white-noise process, the covariance computation is shown to be able to separate the effect of random excitation from the response measurement. Wavelet transform (WT) is then used to convert the response covariance in the time domain to the WT magnitude plot in the time-scale plane. The wavelet coefficients along the curves where energy concentrated can be extracted and used to estimate the modal properties of the structure. These modal property estimations can lead to the calculation of the stiffness matrix when either the spectral density of the random loading or the mass matrix is given. This predicted stiffness matrix hence provides a direct assessment on the possible location and severity of damage which results in stiffness alteration. To demonstrate the proposed wavelet-based damage assessment technique, a numerical example and an experimental study both on a three-story shear-beam building model under a broad-band excitation are presented. Both numerical and experimental results illustrate that the proposed technique can provide an accurate assessment on the damage location. It is however noted that the assessment of damage severity is not as accurate. This might be attributed to the errors associated with the mode shape estimations as well as the assumption of proportional damping adopted in the formulation.

Acknowledgements

This study was supported by the Hong Kong Research Grants Council (Grant No. HKUST6220/01E and 611405), the National Natural Science Foundation of China (Grant No. 50508027 and 50538020), the Major International (Regional) Joint Research Program of the National Natural Science Foundation of China (Grant No. 50420120133), and the Cultivation Fund of the Key Scientific and Technical Innovation Project from the Ministry of Education of China (Grant No. 20041207001). This study was also sponsored by the US National Science Foundation through the International Collaboration grant supplement to CMS-0201320. The guidance of Dr S. C. Liu is gratefully acknowledged.

References

Chang, C.C., Sun, Z. and Li, N. (2003), “Identification of structural dynamic properties using wavelet transform”, *The First International Conference on Structural Health Monitoring and Intelligent Infrastructure,* November 13-15, 2003, Tokyo, Japan.

Delprat, N., Escudie, B., Guillemain, P., Kronland-Martinet, R., Tchamitchian, P. and Torresani, B. (1992), “Asymptotic wavelet and Gabor analysis: Extraction of instantaneous frequencies”, *IEEE Trans. Inform. Theory,* **38:2**, 644-664.

Kijewski, T. and Kareem, A. (2003), “Wavelet transform for system identification in civil engineering”, *Computer-Aided Civil and Infrastructure Engineering*, **18**, 339-355.

Piombo, B. A. D., Fasana, A., Marchesiello, S. and Ruzzene, M. (2000), “Modelling and identification of the dynamic response of a supported bridge”, *Mechanical Systems and Signal Processing,* **14**(1), 75-89.

Peeters, B. and Roeck, G.D. (2001). “Stochastic system identification for operational modal analysis: a review.” *J. Dynamic Systems, Measurement, and Control*, **123**, 659-667.

Ruzzene, M., Fasana, A., Garibaldi, L. and Piombo, B. (1997), “Natural frequencies and dampings identification using wavelet transform: application to real data”, *Mechanical Systems and Signal Processing,* **11:2**, 207-218.

Staszewski, W. J. (1997), “Identification of damping in MDOF systems using time-scale decomposition”, *J. Sound Vib.,* **203**(2), 283-305.

VG